

Targeting Mast Cells and Basophils with Anti-Fc ϵ RI α Fab-Conjugated Celastrol-Loaded Micelles Suppresses Allergic Inflammation

Xia Peng, Juan Wang, Xianyang Li, Lihui Lin, Guogang Xie, Zelin Cui, Jia Li, Yuping Wang, and Li Li*

 Department of Laboratory Medicine, Shanghai First People's Hospital, Medical College,
 Shanghai JiaoTong University, Shanghai 200080, China

Mast cells and basophils are effector cells in the pathophysiology of allergic diseases. Targeted elimination of these cells may be a promising strategy for the treatment of allergic disorders. Our present study aims at targeted delivery of anti-Fc ϵ RI α Fab-conjugated celastrol-loaded micelles toward Fc ϵ RI α receptors expressed on mast cells and basophils to have enhanced anti-allergic effect. To achieve this aim, we prepared celastrol-loaded (PEO-block-PPO-block-PEO, Pluronic) polymeric nanomicelles using thin-film hydration method. The anti-Fc ϵ RI α Fab Fragment was then conjugated to carboxyl groups on drug-loaded micelles via EDC amidation reaction. The anti-Fc ϵ RI α Fab-conjugated celastrol-loaded micelles revealed uniform particle size (93.43 ± 12.93 nm) with high loading percentage ($21.2 \pm 1.5\%$ w/w). The image of micelles showed oval and rod like. The anti-Fc ϵ RI α Fab-conjugated micelles demonstrated enhanced cellular uptake and cytotoxicity toward target KU812 cells than non-conjugated micelles *in vitro*. Furthermore, diffusion of the drug into the cells allowed an efficient induction of cell apoptosis. In mouse model of allergic asthma, treatment with anti-Fc ϵ RI α Fab-conjugated micelles increased lung accumulation of micelles, and significantly reduced OVA-slgE, histamine and Th2 cytokines (IL-4, IL-5, TNF- α) levels, eosinophils infiltration and mucus production. In addition, in mouse model of passive cutaneous anaphylaxis, anti-Fc ϵ RI α Fab-conjugated celastrol-loaded micelles treatment significantly decreased extravasated evan's in the ear. These results indicate that anti-Fc ϵ RI α Fab-conjugated celastrol-loaded micelles can target and selectively kill mast cells and basophils which express Fc ϵ RI α , and may be efficient reagents for the treatment of allergic disorders and mast cell related diseases.

KEYWORDS: Anti-Fc ϵ RI α Antibody Fab Fragment, Celastrol, Polymeric Nanomicelles, Mast Cells, Basophils, Allergic Diseases.

INTRODUCTION

The worldwide prevalence of allergic diseases, including asthma, rhinitis, food allergies, and atopic dermatitis has risen dramatically in recent years. Thus, there is an urgent need for novel and effective therapeutic strategies.¹

Mast cells and basophils are important effector cells in the pathophysiology of allergic diseases. Degranulation of these cells, triggered by the cross-linking of the high-affinity receptor for IgE (Fc ϵ RI), results in the release of allergic and inflammatory mediators that induce the clinical symptoms of type I immediate hypersensitivity.²

Because of their role in triggering the allergic reaction, targeted elimination of mast cells and basophils may be a promising strategy for the treatment of allergic diseases. Previous studies have attempted to eliminate these cells by constructing chimeric proteins. The proteins consisted of a targeting moiety (Fc fragment of IgE) fused to a toxic or pro-apoptotic molecule that serves as a killing moiety. However, the clinical application of such chimeras is restricted due to potential immunogenicity to human organs, non-specific binding with low affinity receptor for IgE, and short half-time in the body.^{3,4}

Traditional Chinese herbal medicine provides a highly solid foundation for modern drug development.⁵ Thunder God Vine, which belongs to the Celastraceae family, has traditionally been used as an antirheumatic. Celastrol, the effective constituent of Thunder God Vine, also

*Author to whom correspondence should be addressed.

Email: annyli@hotmai.com

Received: 8 October 2014

Accepted: 18 February 2015

shows potential for the treatment of autoimmune and chronic inflammatory diseases.^{6,7} Recent studies have demonstrated that celastrol could inhibit mast cell proliferation and induce apoptosis *in vitro*, specifically during S phase, with up-regulation of BAX and c-myc, and down-regulation of Bcl-2.^{8,9} It is widely accepted that cells undergoing apoptosis *in vivo* are recognized and ingested intact by phagocytes, without the release of inflammatory mediators.¹⁰ Therefore, celastrol may exhibit promising efficacy in inhibiting allergic inflammation based on inducing mast cells and basophils apoptosis. However, the low solubility and potential adverse effects on normal organs have hindered the clinical applications of celastrol.

Polymeric micelles have become efficient system for the delivery of a broad variety of hydrophobic drugs.^{11,12} Loading such drugs into the hydrophobic micelle core dramatically increases drug solubility and bioavailability. In our previous study, we developed celastrol-loaded carboxyl-functioned poly(ethylene glycol)-block-poly(propylene glycol)-block-poly(ethylene glycol) (PEO-block-PPO-block-PEO, Pluronic) polymeric nanomicelles, which greatly improved the solubility of celastrol and extended its release.¹³ However, to further prevent undesirable side-effects and increase the drug accumulation in target cells, it is necessary to promote active drug delivery by introducing a target motif on the nanoparticles, enabling them to recognize and bind to specific receptors that are unique to mast cells and basophiles.^{14,15}

The fact that the Fc ϵ RI receptor is mainly distributed on mast cells and basophils makes it an attractive candidate for targeted immunotherapy of allergic disorders. In sensitized individuals, expression of Fc ϵ RI is significantly up-regulated by an increase of IgE levels.¹⁶ As a tetrameric complex, Fc ϵ RI consists of one IgE-binding α -chain, one β -chain and two γ -chains. In recent years, non-degranulation monoclonal antibodies against Fc ϵ RI α (anti-Fc ϵ RI α) and its Fab fragment (anti-Fc ϵ RI α Fab) have been developed for anti-allergic therapy.¹⁷ The anti-Fc ϵ RI α Fab demonstrated to an efficient target motif as it exhibits inhibitory effect to mast cells and basophils, and shows low immunogenicity *in vivo*.

Here, we constructed anti-Fc ϵ RI α Fab-conjugated celastrol-loaded micelles to specially kill mast cells and basophils for targeted allergy treatment. Further, the characteristics of micelles, including particle size, morphology and drug loading percentage, were carried out. The micelles were then evaluated for cellular uptake using confocal microscopy and flow cytometry, *in vitro* cytotoxicity by CCK-8 assay and apoptotic effect using flow cytometry and western blot. Finally, the *in vivo* biodistribution and anti-allergic efficacy were assessed in a mouse model of allergic asthma and passive cutaneous anaphylaxis. This study displayed that anti-Fc ϵ RI α Fab-conjugated celastrol-loaded micelles may be given as new

therapeutic approaches for allergic disorders and mast cell related diseases.

MATERIALS AND METHODS

Materials, Cell Lines, and Animals

Carboxyl-terminated Pluronic P123 copolymer was kindly gifted by Professor DX Cui (Shanghai Jiao Tong University, China). Celastrol (99% purity) was purchased from Nanjing Zelang Pharmaceutical Technology (Nanjing, China). Coumarin 6, 1-(3-Dimethylaminopropyl)-3-ethylcarbodiimide hydrochloride (EDC), and monoclonal anti-dinitrophenyl (anti-DNP) antibody produced in mouse (D8406) were obtained from Sigma-Aldrich (Shanghai, China). Penicillin, streptomycin, RPMI 1640 and fetal bovine serum (FBS) were purchased from Gibco BRL (California, USA). CCK-8 and caspase 3 activity kit (C1115) were purchased from Beyotime® Biotechnology (Nantong, China). Annexin V-FITC Apoptosis Detection Kit was purchased from Life Technologies Corporation (California, USA). Rabbit anti-human PARP antibody and Horseradish peroxidase (HRP)-conjugated goat anti-rabbit-IgG (H and L) secondary antibody were obtained from Cell Signaling Technology (Shanghai, China). Chemiluminescence phototope-HRP Kit was purchased from Millipore (Massachusetts, USA). DNP-HAS (sc-396282) was purchased from Santa Cruz (Dallas, USA). Mouse anti-OVA-IgE ELISA Kit (AKRIE-030) was purchased from Shibayagi (Gunma, Japan). Histamine ELISA kit (BAE-100) was obtained from LDN (Nordhorn, Germany). All other reagents were purchased from Sigma-Aldrich (Shanghai, China).

Human basophil cell line KU812 cells which expressed Fc ϵ RI α on their surface and immature human mast cells line HMC-1 cells which did not express Fc ϵ RI α were cultured in RPMI 1640 medium supplemented with 10% heat-inactivated FBS, 100 U/mL penicillin, 10 mg/mL streptomycin, and 2 mmol/L L-glutamine containing at 37 °C, 5% CO₂.

Specific pathogen-free female BALB/c mice (6–8 weeks old) were obtained from Sion-British Sippr/BK Laboratory. All animal experiments were conducted in the Laboratory Animal Research Center of the Second Military Medical University, and were approved by Chancellor's Animal Research Committee.

Monoclonal Antibody Preparation

The monoclonal antibody (mAb) was prepared against Fc ϵ RI α on human mast cells and basophils. We obtained the mAb from mouse hybridoma cell lines using the standard method of Koehler and Milstein.¹⁸ The antibody was purified by affinity chromatography on protein G-Sepharose (Pharmacia, Uppsala, Sweden). The anti-Fc ϵ RI α Fab was isolated by digestion with papain and purified with affinity chromatography.

Preparation of Anti-Fc ϵ RI α Fab-Conjugated Celastrol-Loaded Micelles

Carboxyl-terminated Pluronic P123 nanomicelles filled with celastrol were prepared using the thin-film hydration method under optimized conditions as described previously.¹³ For covalent attachment of anti-Fc ϵ RI α Fab onto the micelle surface, EDC chemistry was employed.^{19,20} Briefly, the celastrol-loaded micelles were incubated with 100 mM EDC for 30 min. Then the activated carboxyl groups on the surface of micelles were allowed to react with the amino terminus of monoclonal anti-Fc ϵ RI α antibody Fab fragment (0.71 mg/mL) for 2 h at room temperature. The resultant anti-Fc ϵ RI α Fab-conjugated celastrol-loaded micelles (anti-Fc ϵ RI α Fab-NMs-celastrol) were subsequently freeze-dried for 24 h (FD-1A-50, Biocool, Beijing, China) at a condenser temperature of -52°C and pressure of less than 0.1 Mbar. The freeze-dried samples were stored at -20°C and were rehydrated to achieve the required concentration of celastrol with PBS for further experiments.

Characterization of Micelles

Particle size and morphology of celastrol-loaded non-conjugated and anti-Fc ϵ RI α Fab-conjugated celastrol-loaded micelles was analyzed by Dynamic light scattering (DLS) analyses and transmission electron microscope (TEM), respectively, as described previously.¹³

Drug Loading Level

The amount of celastrol in the micelle formulations was detected using a reversed phase HPLC on an Agilent 1100 series HPLC system as described previously.¹³

Binding and Uptake of Micelles by KU812 Cells

For cellular uptake assay, coumarin 6 was entrapped into the hydrophobic core of the Pluronic P123 nanomicelles instead of the celastrol. The preparation of coumarin 6-loaded micelles and anti-Fc ϵ RI α Fab-conjugated coumarin 6-loaded micelles (Pluronic P123 copolymers: coumarin 6 = 4000:1, w/w) were the same procedures with those of celastrol-loaded micelles and anti-Fc ϵ RI α Fab-conjugated celastrol-loaded micelles, respectively. After dissolution of micelles in chloroform, the level of encapsulated coumarin 6 in micelles was evaluated by fluorophotometer (HITACHI F4600, Tokyo, Japan) with an excitation wavelength of 460 nm and emission wavelength of 501 nm.

KU812 and HMC-1 cells were collected at a density of 5×10^5 cells/mL, washed twice with PBS, and incubated with 0.2 mL of coumarin 6-loaded anti-Fc ϵ RI α Fab-conjugated and non-conjugated micelles at 37°C for 2 h. After incubation, cells were fixed with formaldehyde (4% in PBS) for 10 min at 25°C , and stained with DAPI for 10 min at 25°C . After washing with PBS twice, the cells were resuspended with 100 μL PBS, and added

to confocal dishes. Images were observed and captured using confocal laser scanning microscopy (CLSM) with a $63 \times$ oil immersion objective (Leica TCS SP5II, Jena, Germany). Fluorochromes were excited at 488 nm for coumarin 6 and at 360 nm for DA PI.

Flow cytometry was also used to examine the cellular uptake of the coumarin 6-loaded anti-Fc ϵ RI α Fab-conjugated or non-conjugated micelles. Cells were collected and incubated with micelles as described above. After incubation for 2 h, cells were washed twice with PBS, and suspended in PBS containing 1% BSA. The intensity of the coumarin 6 fluorescence in the cells was determined on a FACS Calibur (FC500, Beckman Coulter, Miami, FL, USA) using excitation and emission settings of 488 nm and 535 nm (Fl-1 channel). The data was analyzed by Beckman FACS analysis software. The experiments were run in triplicate and repeated three times with similar results.

In Vitro Cytotoxicity Study

K U812 and HMC-1 cells were seeded at a density of 4×10^4 cells per well in 96-well plates. After 2 h of incubation at 37°C with 5% CO₂, cells were treated with 50 μL of drug free anti-Fc ϵ RI α Fab-conjugated micelles (anti-Fc ϵ RI α Fab-NMs), drug free non-conjugated micelles (NMs), free celastrol in DMSO, celastrol-loaded micelles (celastrol-NMs), and anti-Fc ϵ RI α Fab-conjugated celastrol-loaded micelles (anti-Fc ϵ RI α Fab-NMs-celastrol) in different celastrol concentrations for 24 h. Cell proliferation was then measured using CCK-8 assay. Briefly, 15 μL of CCK-8 solution were added to each well, and then the plate was incubated for an additional 3 h at 37°C , the absorbance at 450 nm was measured using a microplate reader (Molecular Devices, Menlo Park, CA, USA).

Cell Apoptosis Assay

Apoptosis induction was determined using Dead Cell Apoptosis Kit (Invitrogen), caspase-3 and poly(ADP ribose) polymerase (PARP) activity measurement. An early indicator of apoptosis is the rapid translocation and accumulation of the membrane phospholipid phosphatidylserine from the cytoplasmic interface to the extracellular surface. This loss of membrane asymmetry can be detected by Annexin-V staining. In brief, 5×10^5 cells were pre-treated with NMs, free celastrol in DMSO, celastrol-NMs, and anti-Fc ϵ RI α Fab-NMs-celastrol for 24 h, after incubation, cells were washed twice with PBS, and then labeled with Annexin V-FITC and PI in binding buffer according to the instructions provided by the manufacturer in the Annexin V-FITC Apoptosis Detection Kit. Analysis was done by flow cytometry (FC500, Beckman Coulter, Miami, FL, USA).

For caspase-3 activity measurement, cells were washed with PBS and lysed. The activity levels were determined using specific caspase colorimetric assay kits.

PARP cleavage was evaluated by Western blot. Briefly, cell lysates (30 μ g) were equally loaded on 8% SDS-polyacrylamide gel for separation and then transferred to PVDF membranes. Membranes were blocked with 5% nonfat milk in TBST, and then incubated overnight with rabbit mAb against PARP. After staining with horseradish peroxidase (HRP)-linked goat anti-rabbit-IgG secondary antibody, signal detection was performed using a chemiluminescence phototope-HRP Kit. The signal of the target protein was detected using the Chemi Doc MP imaging system (Bio-Rad, Munich, Germany).²¹

Model of Allergic Sensitization and Challenge with Ovalbumin

Mice were sensitized with intraperitoneal injections of 20 μ g of ovalbumin (OVA) absorbed to 4 mg of Al(OH)₃ on days 0, 7 and 14. The negative control mice were sensitized with PBS. From days 21 to 25 the mice were nebulized with 2% OVA for 20 min once daily for 5 consecutive days (local challenge) using a nebulizer (Yuwell, Jiangsu, China) and the control mice were nebulized with PBS at the same times (see Fig. 2).²²

In Vivo Distribution of Micelles in Mouse Model of Allergic Asthma

To investigate the lung targeting efficiency of micelles *in vivo*, DiR (Fanbo, Beijing, China), a near-infrared fluorescent dye, was encapsulated in the carboxyl-modified Pluronic P123 micelles. Briefly, 10 μ g of DiR were co-dissolved with 4 mg of carboxyl-modified Pluronic P123 copolymer in dichloromethane. After forming micelles, the free DiR was removed by centrifugation at 8000 rpm for 5 min. BALB/c mice were sensitized and challenged with OVA, and randomly assigned into two groups ($n = 6$ mice per group), and injected intraperitoneally (i.p.) with either DiR-loaded micelles or anti-Fc ϵ RI α Fab-conjugated DiR-loaded micelles at the same DiR concentrations. After 3 and 6 h, mice were killed by cervical dislocation ($n = 3$ at each point), and the tissues (liver, kidney, spleen, heart, lung, and brain) were isolated and washed in normal saline. Time-course fluorescent images (excitation: 720/20 nm; emission: 790/30 nm; integration time: 15 s) were acquired on a Bruker *In-Vivo* F PRO imaging system (Billerica, MA, USA). The acquired images were measured and analyzed with Living Imaging software (Billerica, MA, USA).

The Anti-allergic Activity of Anti-Fc ϵ RI α Fab-Conjugated Celastrol-Loaded Micelles in Mouse Model of Allergic Asthma

To investigate the anti-allergic activity of anti-Fc ϵ RI α Fab-conjugated celastrol-loaded micelles, 300 μ L of free celastrol in DMSO, celastrol-NMs, and anti-Fc ϵ RI α Fab-NMs-celastrol were administered i.p. at the celastrol concentration of 0.8 mg/kg for 5 consecutive days from

day 21 to 25. Drugs were given 1 hour before every local challenge. An equal quantity of normal saline was administered to asthmatic and control mice. All mice were euthanized on the following day (day 26).

Determination of Serum OVA Specific IgE

Blood samples were collected immediately after cervical dislocation by retro-orbital bleeding, allowed to clot at room temperature, and then centrifuged at 5000 rpm for 10 min. Aliquots of serum were stored at -70 °C until analyzed for serum OVA-specific IgE (OVA-sIgE) with mouse anti-OVA-IgE ELISA Kit.

Determination of Cytokines and Histamine in BALF

Immediately after euthanization, the lungs were lavaged by flushing 300 μ L of cold PBS through the trachea three times. Bronchoalveolar lavage fluid (BALF) was collected and centrifuged at 4 °C. The supernatant of BALF was stored at -80 °C for measuring histamine and cytokine production.

Productions of interleukin (IL)-4, IL-5, IL10, IL-13, tumor necrosis factor (TNF)- α , and interferon (IFN)- γ in the BALF were determined by 6-plex Luminex assay (ProcartaPlex Mouse Th1/Th2 cytokine Panel, eBioscience, California, USA). Levels of histamine in the BALF samples were measured with histamine ELISA Kit.

Histological Examination

The non-lavaged lung was removed and fixed in 10% neutral-buffered formalin for 24 h. Lung tissues were embedded in paraffin and sectioned at 5 μ m. Tissue sections were then stained with hematoxylin 8 and eosin (H and E) and PAS. Images were obtained under light microscopy at 20 \times magnification. Peribronchial and perivascular inflammation were assessed by a blinded observer.

Effect of Anti-Fc ϵ RI α Fab-Conjugated Celastrol-Loaded Micelles on Passive Cutaneous Anaphylaxis

For passive cutaneous anaphylaxis (PCA), BALB/c mice were injected with PBS, free celastrol in DMSO, celastrol-NMs, and anti-Fc ϵ RI α Fab-NMs-celastrol intravenously at the celastrol concentration of 1.5 mg/kg 24 hours before challenge. Mouse IgE anti-DNP was injected intradermally into the left ear cartilage (pinna), and PBS was injected into the right pinna 2 hours before intravenous challenge with 300 mg of DNP-HSA in 1% Evans Blue dye. After 40 minutes, mice were euthanized. The pinnae were then removed, and incubated at 25 °C overnight in 2 mL of acetone with 0.5% sodium sulfate. After incubation, the solution was centrifuged at 5000 rpm for 5 min, and the supernatant was collected. The extravasated blue dye was detected at 620 nm.

Statistical Analysis

Statistical analyses were performed using GraphPad Prism Software (GraphPad Software, La Jolla, CA) or SPSS 17.0 (SAS Institute, Cary, North Carolina, USA). Statistical significance of differences in all measurements between control and treated groups was determined by a one-way ANOVA followed by a Dunnett's or Tukey's HSD test for multiple-group analysis. Student's paired *t* test was used for pairwise group comparisons, as needed. Values of *P* < 0.05 were considered to indicate significant differences.

RESULTS

Characterization of Micelles

The anti-Fc ϵ RI α Fab-conjugated celastrol-loaded micelles (anti-Fc ϵ RI α Fab-NMs-celastrol) were synthesized as shown in Figure 1. According to DLS measurements, particle size of micelles was slightly increased (from 85.53 nm to 94.43 nm) after conjugation with anti-Fc ϵ RI α Fab. Both anti-Fc ϵ RI α Fab-conjugated and non-conjugated celastrol-loaded micelles exhibited a narrow size distribution (*PI* < 0.2). Besides, drug loading percentage was not

affected by conjugation with anti-Fc ϵ RI α Fab on micelles (Table I). TEM image of anti-Fc ϵ RI α Fab-NMs-celastrol showed oval and rod like (Fig. 2), which was similar to that of celastrol-loaded non-conjugated micelles (celastrol-NMs).¹⁶ Taken together, Surface modified micelles by anti-Fc ϵ RI α Fab had a negligible effect on its physical characteristics.

In Vitro Cellular Uptake

To determine the effect of anti-Fc ϵ RI α Fab conjugation on cellular uptake, cells were treated with coumarin 6-loaded anti-Fc ϵ RI α Fab-conjugated and non-conjugated micelles, and the cellular fluorescence was detected by flow cytometry and confocal microscopy. The anti-Fc ϵ RI α Fab-conjugated micelles showed a stronger uptake by KU812 cells which expressed Fc ϵ RI α (target cell), than that of non-conjugated micelles indicated as a stronger right shift along the *x*-axis of the histogram (Fig. 3(A)). As expected, anti-Fc ϵ RI α Fab-conjugated micelles introduced to HMC-1 cells which did not express Fc ϵ RI α (non-target cell), showed no increase in cellular uptake compared with non-conjugated micelles (Fig. 3(B)).

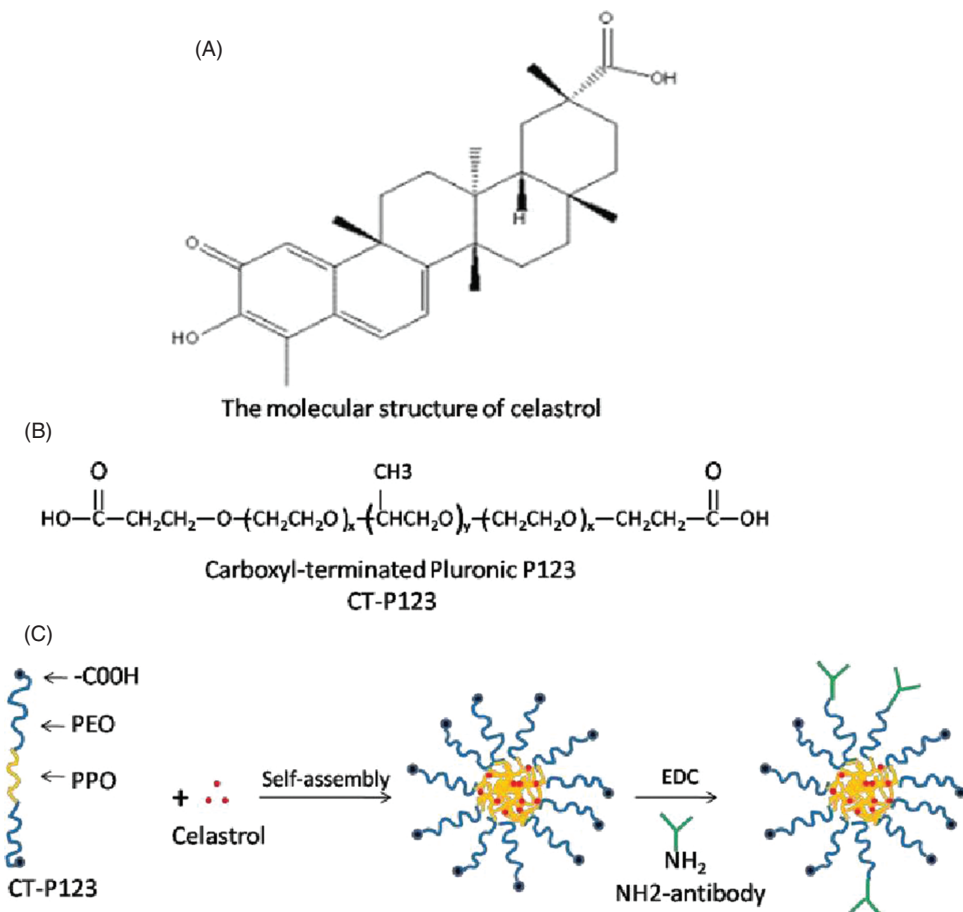


Figure 1. Preparation of anti-Fc ϵ RI α Fab-conjugated celastrol-loaded micelles. (A) The molecular structure of celastrol, (B) Schematic structure of carboxyl-terminated Pluronic P123 copolymer, (C) coupling of amino group-containing ligands (antibodies) with carboxyl groups on micelles.

Table I. Characteristics of prepared polymeric micelles ($n = 3$).

Micelles	Particle size (nm)	Polydispersity (PI)	Drug loading percentage (%)
Celastrol-NMs	85.53 ± 7.23	0.18 ± 0.03	22.8 ± 1.0
Anti-FcεRIα Fab-NMs-celastrol	93.43 ± 12.93	0.14 ± 0.01	21.2 ± 1.5

The cellular uptake was further investigated by confocal microscopy. KU812 cells demonstrated an apparent increase in fluorescence intensity for anti-FcεRIα Fab-conjugated micelles over the non-conjugated micelles (Fig. 3(C)), whereas both anti-FcεRIα Fab-conjugated and non-conjugated micelles introduced to HMC-1 cells showed very weak coumarin 6 fluorescence (Fig. 3(D)). It could be seen that the uptake of micelles by cells which express FcεRIα receptor, significantly increased with anti-FcεRIα Fab conjugation. However, anti-FcεRIα Fab conjugation did not influence cellular uptake of micelles for cells which do not have FcεRIα receptor.

In Vitro Cytotoxicity

The effects of different celastrol formulations on the proliferative ability of KU812 and HMC-1 cells were studied at 24 h post-treatment using CCK-8 assay. Drug-free anti-FcεRIα Fab-conjugated (anti-FcεRIα Fab-NMs) and non-conjugated micelles (NMs) did not show any cytotoxicity toward KU812 cells, and celastrol-NMs and free celastrol caused cell killing in a dose-dependent manner, whereas anti-FcεRIα Fab-NMs-celastrol provoked a higher cell death at the same celastrol concentration (2 to 8 μ M) (Fig. 4(A)). The IC₅₀ value of anti-FcεRIα Fab-NMs-celastrol ($1.33 \pm 0.09 \mu$ M, $n = 3$) was lower than that for celastrol-NMs ($2.03 \pm 0.12 \mu$ M, $n = 3$) ($p < 0.05$) and

free celastrol ($2.5 \pm 0.13 \mu$ M, $n = 3$) ($p < 0.05$) in KU812 cells. This result suggested that anti-FcεRIα Fab enhanced the cytotoxicity of micelles to target cells. No differences in cytotoxicity of anti-FcεRIα Fab-NMs-celastrol, celastrol-NMs, and free celastrol at the same celastrol concentration of celastrol (2 to 8 μ M) were observed in HMC-1 cells (Fig. 4(B)). Besides, the IC₅₀ value for anti-FcεRIα Fab-NMs-celastrol ($2.46 \pm 0.18 \mu$ M, $n = 3$) in HMC-1 cells was higher than that in KU812 cells ($p < 0.05$). Taken together, these data confirmed that target cells were more sensitive to anti-FcεRIα Fab-NMs-celastrol than non-target cells.

Cell Apoptosis

To further confirm the celastrol induced apoptosis, KU812 cells were treated with various celastrol formulations at 2 μ M for 24 h, and the apoptosis of cells were measured by flow cytometry using Annexin-V and PI staining. The percentage of apoptosis of anti-FcεRIα Fab-NMs-celastrol (41.5%) treated cells was higher compared with that of the celastrol-NMs (30.5%) ($p < 0.05$) and free celastrol (25.0%) treated cells ($p < 0.05$) (Figs. 5(A, B)).

To further support the above results, we also analyzed PARP and caspase-3 activation, a hallmark of the apoptosis induction. As shown in Figures 5(C, D), anti-FcεRIα Fab-NMs-celastrol treatment induced an increased caspase-3 activity and cleavage of PARP, suggesting that the anti-proliferative and cytotoxic effects of anti-FcεRIα Fab-NMs-celastrol could be attributed, at least in part, to the activity of these apoptosis mediators.

In Vivo Biodistribution of Micelles in Mouse Model of Allergic Asthma

To evaluate whether micelles conjugated with anti-FcεRIα Fab result in measurable increases in lung fluorescence in mouse model of allergic asthma, DiR-loaded anti-FcεRIα Fab-conjugated and non-conjugated micelles were injected intraperitoneally, and then *ex vivo* imaging of major organs was performed. As shown in Figure 6, the fluorescence was mainly seen in liver, spleen and kidney after injection with anti-FcεRIα Fab-conjugated and non-conjugated micelles both at the 3 h and 6 h time points. At the 3 h time point, the DiR fluorescence intensity in lung isolated from anti-FcεRIα Fab-conjugated micelles-treated mice was slightly stronger compared to that in lung isolated from non-conjugated micelles-treated mice. Surprisingly, the kidney fluorescence was also enhanced in anti-FcεRIα Fab-conjugated micelles-treated group. Six hours after injection, the lung fluorescence in anti-FcεRIα Fab-conjugated micelles-treated mice was much more obvious than that in anti-FcεRIα Fab-non-conjugated micelles-treated group. Simultaneously, less DiR fluorescence in spleen and kidney was observed in anti-FcεRIα Fab-conjugated micelles-treated mice than that in control group. This result indicated that anti-FcεRIα

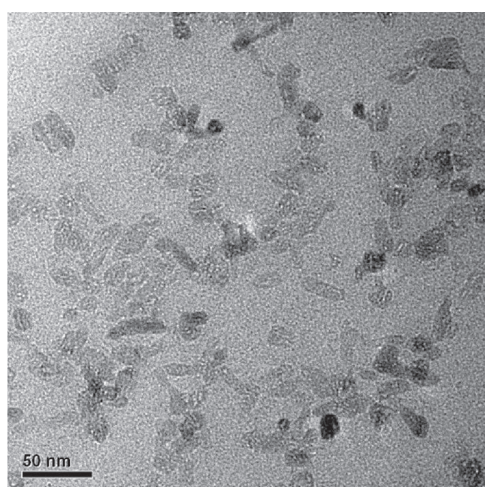


Figure 2. TEM graph of anti-FcεRIα Fab-conjugated celastrol-loaded micelles.

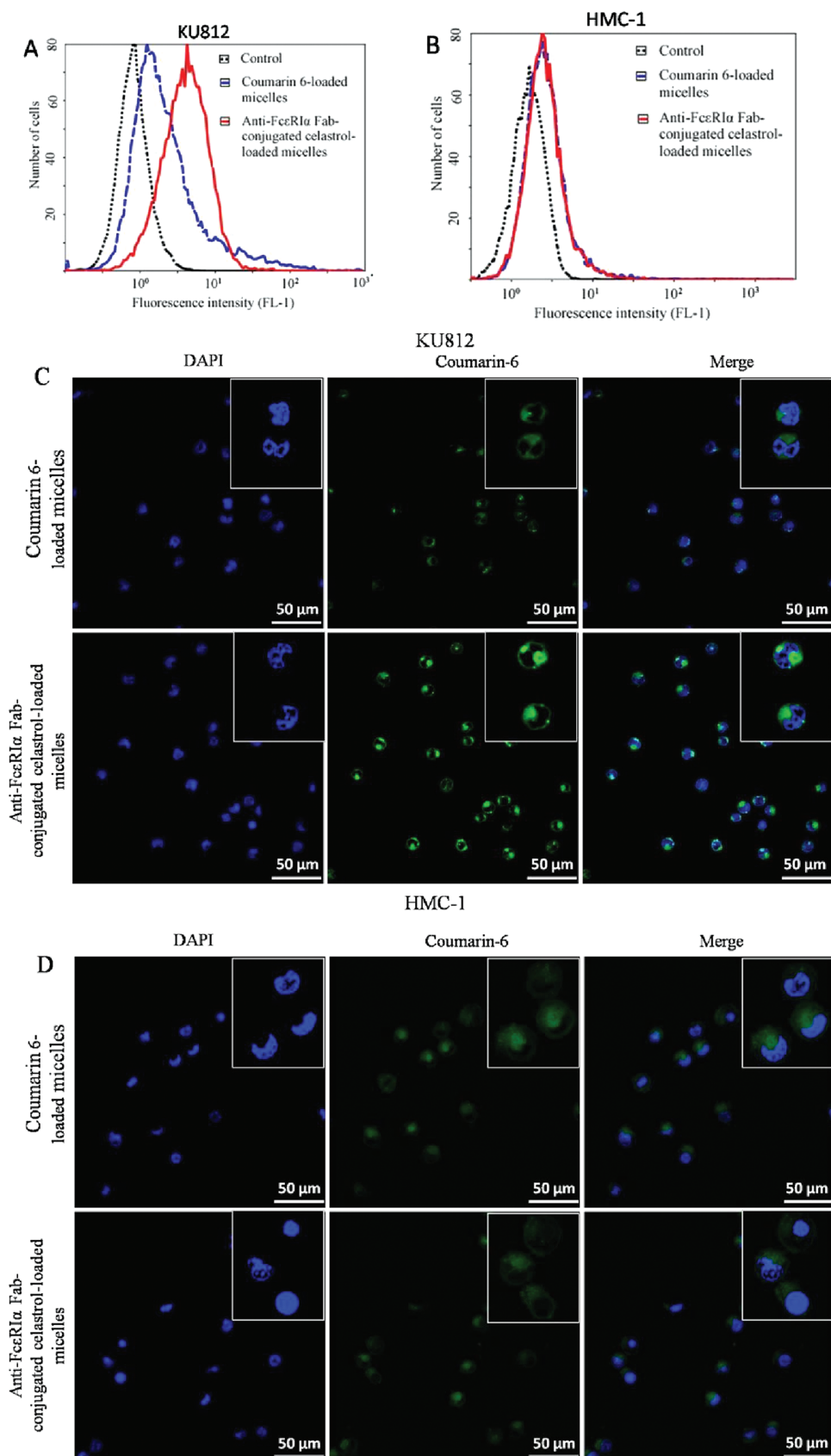


Figure 3. CLSM ((A) and (B)) and FACS histogram ((C) and (D)) of the uptake of coumarin 6-loaded anti-Fc ϵ RI α Fab-conjugated and non-conjugated micelles after incubation with KU812 and HMC-1 cells for 2 h at 37 °C. The magnification bar is 50 μ m.

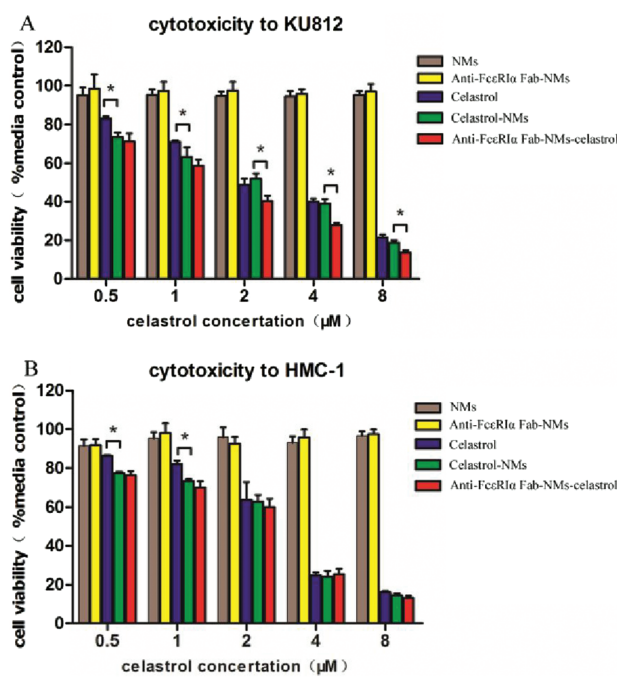


Figure 4. Cytotoxicity of various celastrol formulations toward KU812 (A) and HMC-1 cells (B) after incubation with anti-FcεRIα Fab-NMs-celastrol and various controls, including free celastrol in DMSO, celastrol-NMs, anti-FcεRIα Fab-NMs and NMs for 24 h at 37 °C (* $p < 0.05$, mean \pm SD, $n = 3$).

Fab-conjugated micelles could assist the encapsulated drug targeted to the lung in mouse model of allergic asthma.

Inhibition of OVA-Mediated Airway Allergic Reactions by Micelles

Since anti-FcεRIα Fab enhanced the effect of celastrol-loaded micelles *in vitro*, we determined the anti-allergic effect of anti-FcεRIα Fab-NMs-celastrol in a mouse model of allergic asthma. Different celastrol formulations were administrated as in Figure 7. Although native celastrol and celastrol-NMs could alleviate allergic airway inflammation, a much more efficient inhibition of allergic reactions was obtained with anti-FcεRIα Fab-NMs-celastrol therapy.

Antigen-mediated allergic responses are known to induce Th2-specific Ig production such as antigen-specific IgE antibody.²³ Thus, we examined whether anti-FcεRIα Fab-NMs-celastrol influenced OVA-specific IgE (OVA-sIgE) concentration. OVA challenge (31.53 ± 4.87 U/mL) resulted in an increase of OVA-sIgE, compared to controls (1.66 ± 0.11 U/mL) ($p < 0.05$). IgE level was decreased after injection of different celastrol formulations. However, a greater reduction in OVA-sIgE level was achieved with anti-FcεRIα Fab-NMs-celastrol treatment (73%) in comparison of both celastrol-NMs (46%) ($p < 0.05$) and free celastrol (13%) ($p < 0.05$) treatment (Fig. 8(A)).

In addition, we analyzed the histamine level in BALF, which can increase the permeability of the capillaries to promote inflammatory cell infiltration.²⁴ Treatment with anti-FcεRIα Fab-NMs-celastrol significantly diminished the level of histamine in response to OVA. In comparison with saline treatment group, 62.5% of histamine was decreased with anti-FcεRIα Fab-NMs-celastrol treatment, and only 28.7% and 25% were reduced with celastrol-NMs and free celastrol treatment, respectively (Fig. 8(B)).

Th1 and Th2 cytokines have been known to induce allergic inflammation and cause early phase asthma.²⁵ Therefore, we further explored the cytokine levels in BALF. OVA challenge increased levels of IL-4, IL-5, IL-13 and TNF- α , all characteristic Th2 cytokines that promote allergic inflammation, and decreased the level of anti-inflammatory cytokine IL-10. IL-4, IL-5 and TNF- α levels were reduced more significantly in anti-FcεRIα Fab-NMs-celastrol treated mice than in celastrol-NMs or native celastrol treated group, whereas IL-10 was elevated with anti-FcεRIα Fab-NMs-celastrol treatment (Fig. 8(D)). Besides, the level of Th1 cytokine IFN- γ remained unchanged.

We also examined the pulmonary infiltration of inflammatory cells, a critical characteristic in allergic inflammation. OVA challenge increased the amount of total inflammatory cells, eosinophils and neutrophils in BALF. A reduction in the amount of these inflammation cells was observed in mice treated with various celastrol formulations. Among all the treatment groups, anti-FcεRIα Fab-NMs-celastrol treated mice demonstrated the fewest inflammatory cells in BALF (Fig. 8(C)). Histological analysis of lung tissue sections revealed that mice challenged with OVA exhibited severe pulmonary infiltration of eosinophil around the bronchial and perivascular areas (Fig. 9(A)), as well as excess mucus production (Fig. 9(B)). These features were almost suppressed in mice treated with anti-FcεRIα Fab-NMs-celastrol, and slightly inhibited in those treated with celastrol-NMs and native celastrol.

Inhibition of Passive Cutaneous Anaphylaxis by Micelles

To further confirm the *in vivo* anti-allergic effect of micelles, we performed PCA reaction after injection of different celastrol formulations to mice, and then evan's blue extravasation was detected. We assumed that if anti-FcεRIα Fab-NMs-celastrol was cytotoxic to mast cells, it would be able to prevent or diminish the PCA reaction. As shown in Figures 10(A, B), Treatment with different celastrol formulations could inhibit PCA reaction. However, mice injected with anti-FcεRIα Fab-NMs-celastrol exhibited less extravasated evan's blue than that treated with celastrol and celastrol-NMs. Similar results were obtained when different celastrol formulations were administrated in the back skin (data not shown).

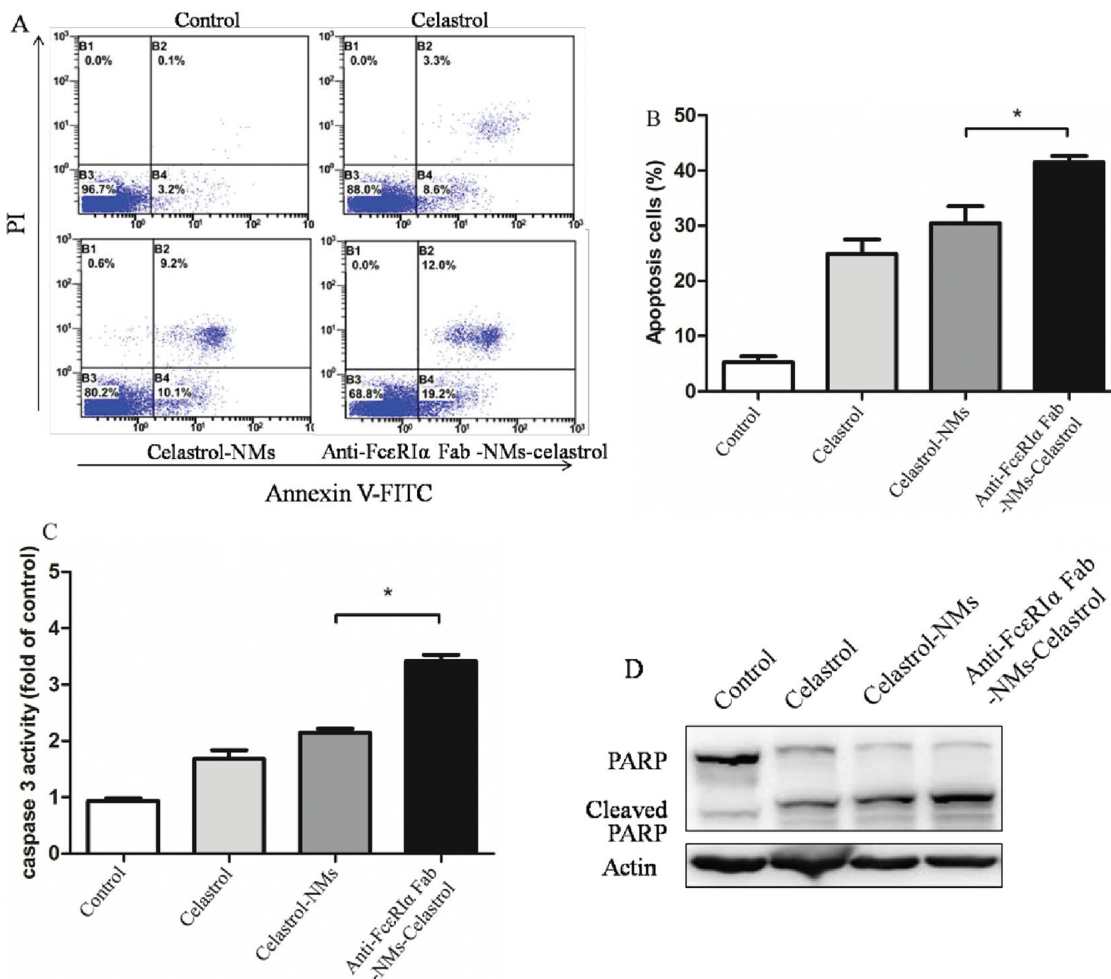


Figure 5. Effect of different celastrol formulations on apoptosis of KU812 cells. (A) FACS analysis of apoptotic cells induced by PBS, anti-FcεRI Fab-NMs-celastrol, celastrol-NMs and free celastrol after 24 h treatment. (B) The number of apoptotic cells in different groups (* $p < 0.05$, mean \pm SD, $n = 3$). (C) Caspase-3 activity. Data are expressed in fold of controls (* $p < 0.05$, mean \pm SD, $n = 3$). (D) Western blot analysis performed using antibodies specific to PARP. β -actin was used as a loading control.

DISCUSSION

Mast cells and basophils are the primary initiating cells of immediate hypersensitivity reactions. Therefore, effective targeted elimination of mast cells and basophils is expected to be a powerful approach to the treatment of allergic diseases. In this context, we constructed anti-FcεRIα Fab-conjugated celastrol-loaded micelles to inhibit allergic inflammation based on specially inducing mast cells and basophils apoptosis. The micelles were about 100 nm by DLS with impressively high drug loading ($21.2 \pm 1.5\%$). However, the particle size of micelles detected by TEM was smaller than that by DLS, which was similar to the results reported by Prathna.²⁶ The reason may be that the two methods are based on different sample preparation processes and different principles. DLS determines particle size of nanoparticles in colloidal solution, while TEM determines that of dehydrated nanoparticles.¹³ TEM showed that micelles were oval and rod like. The structure may be formed for

that the long hydrophobic chains of block copolymer shrink easily and the hydrocarbon chains are more ordered in rod-shaped micelles compared to spherical micelles.²⁷

The targeting effect of anti-FcεRIα Fab-NMs-celastrol was investigated on human basophil cell line KU812 cells which expressed FcεRIα and immature human mast cell line HMC-1 cells which did not express FcεRIα on its surface.^{28,29} Both FACS and CLMS results suggested that anti-FcεRIα Fab conjugation enhanced the cellular uptake of celastrol in target KU812 cells, but not in non-target HMC-1 cells (Fig. 3). Diffusion of the drug into the cells allowed an efficient induction of cell apoptosis. Here, free celastrol demonstrated lower apoptotic efficiency in target KU812 cells than celastrol-NMs and anti-FcεRIα Fab-NMs-celastrol, which was contrary to results observed by Wang et al.³⁰ This could be explained by differences in the cellular uptake mechanism. The uptake of free celastrol may be achieved by diffusion of drug molecules across

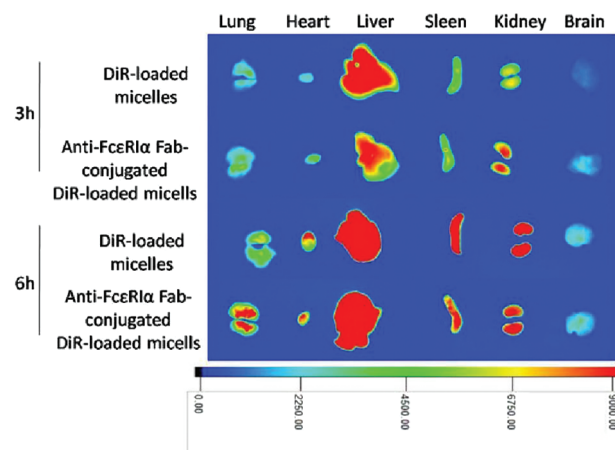


Figure 6. Representative *ex vivo* fluorescence image of major organs from mice euthanized at the indicated times after i.p. injection of DiR loaded anti-Fc ϵ RI α Fab-conjugated and non-conjugated micelles.

cell membrane, which rapidly reaches saturation. Then the small fraction of free celastrol diffused into cytoplasmic compartment is responsible for the apoptosis of KU812 cells.³¹ The transportation of celastrol in celastrol-NMs may be achieved either by diffusion following their release from the micelles or by non-specific endocytosis of the drug loaded micelles.³² Then the internalized celastrol-loaded micelles seem to remain in the cytoplasm and release the encapsulated celastrol in a sustained manner as the polymer degrades slowly. Hence, celastrol-NMs showed stronger therapeutic efficiency over free celastrol. The higher apoptosis-inducing activity of the anti-Fc ϵ RI α Fab-NMs-celastrol in our study was mainly achieved by Fc ϵ RI α -mediated endocytosis, which aids in the intracellular accumulation of the micelles.

Our previous studies showed that anti-Fc ϵ RI α Fab revealed high affinity binding to bone marrow-derived mast cells (BMMC) induced by SCF and IL-3, which demonstrated the cross-reactivity of anti-Fc ϵ RI α Fab

with mouse Fc ϵ RI α (unpublished data), hence facilitating *in vivo* evaluation of anti-Fc ϵ RI α Fab conjugated micelles.

The *in vivo* effects of micelles were investigated using mast cell-dependent mouse models of allergic asthma and passive cutaneous anaphylaxis. Firstly, we evaluated the *in vivo* targeting effect and anti-allergic efficacy of micelles in a mouse model of allergic asthma.^{33,34} Allergic asthma is an inflammatory disease of the airway, characterized by lung mastocytosis and pulmonary inflammation. The pathology observed in allergic asthma is induced by mast cell activation and mediator release independently, as well as in concert with other immune cells. Mast cell mediators such as histamine and leukotrienes contribute to eosinophil recruitment, and mast cell-derived cytokines can cause B cells to class switch to synthesize IgE, recruit inflammatory cells, and promote the development of T cells into a Th2 phenotype.^{35,36} Considering the role of mast cells in allergic asthma, we assume that if anti-Fc ϵ RI α Fab-NMs-celastrol is especially cytotoxic to mast cells, it would be able to accumulate in the lung and alleviate the allergic inflammation.

In vivo distribution of micelles in a mouse model of allergic asthma showed that micelles tended to accumulate in liver, spleen and kidney. The reasons may be that micelles ranging 100–150 nm were preferentially taken up in the liver by the reticuloendothelial system (RES), especially in liver and spleen.³² Meanwhile, kidney accumulation of micelles was also observed. This result may be explained by the biological properties of Pluronic P123. It was reported earlier that Pluronics were excreted primarily through the kidneys.³⁷ However, at the 3 h time point, kidney fluorescence was stronger in anti-Fc ϵ RI α Fab-conjugated micelles-treated group than that in non-conjugated micelles-treated group. Since there was no difference in particle size and drug loading percentage between the two micelles (Table I), the different distribution of the two micelles in kidney during the 3 h may be attributed to different charge on the surface of micelles. Our previous result demonstrated that the pI of antibody used in this research was about 8.0, which makes antibody carry cationic in blood (pH = 7.35–7.45). It was also reported previously that celastrol-loaded micelles were inherently negatively charged. Therefore, antibody conjugated micelles carried less anion than non-conjugated micelles. Since filtration membrane in the kidney is covered with a layer of the negatively charged sialic acid, antibody conjugated micelles which carry less anion may accumulate more in the kidney than non-conjugated micelles in 3 h. Anyway, our results demonstrated that anti-Fc ϵ RI α Fab enhanced the accumulation of micelles in the lung, which may be attributed to the pulmonary mastocytosis in allergic mice.

In asthmatics, pulmonary inflammatory is characterized by abnormal shift of Th1/Th2 balance in favor of Th2 cells, infiltration of eosinophils and lymphocytes, and

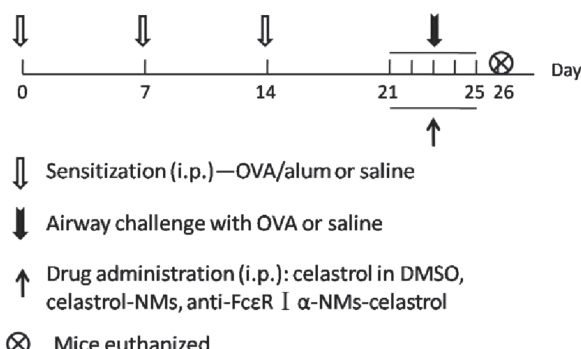


Figure 7. The experimental design. Schematic representation of the experimental protocol for allergic sensitization and challenge with OVA in BALB/c mice. At the end of the experiments, blood and lungs were collected for further analysis.

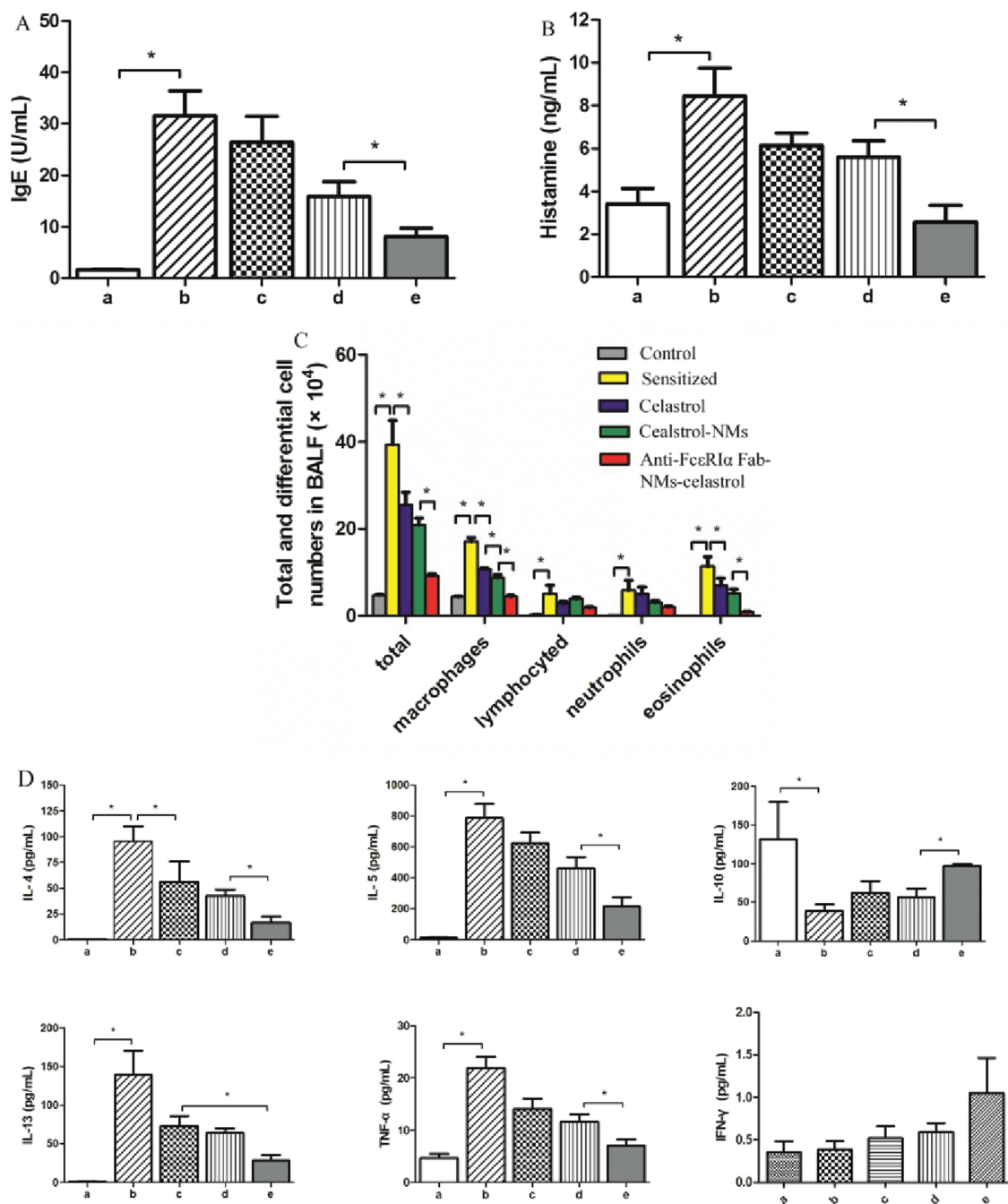


Figure 8. Effect of different celastrol formulations on IgE production, allergic mediator release and inflammatory cell infiltration in a mouse model of allergic asthma. Serum and BALF cell samples were obtained from different groups ((a) non-sensitized mice treated with PBS, (b) sensitized mice treated with PBS, (c) sensitized mice treated with celastrol, (d) sensitized mice treated with celastrol-NMs, (e) sensitized mice treated with anti-Fc ϵ RI α Fab-NMs-celastrol). Serum OVA-sIgE (A) and BALF histamine (B) levels were detected by ELISA. (C) Total BALF cells was counted by counting plate and differential counts of BALF cells (macrophages, lymphocytes, neutrophils and eosinophils) were determined by counting 300 cells on cytospin slides stained with Wright-Giemsa using morphological criteria. (D) Concentrations of cytokines (IL-4, IL-5, IL-10, IL-13, TNF- α , and IFN- γ) in BALF were assessed by Luminex assay. Results are reported as the mean \pm SD ($n = 8$), * $p < 0.05$.

secretion of mucus.^{38,39} Our study suggested that OVA challenge successfully induce a typical Th2 response in the absence of Th1 response, with strong production of OVA-sIgE, increase of Th2 pro-inflammatory cytokines

(IL-4, IL-5, IL-13, and TNF- α) and decrease of anti-inflammatory cytokine (IL-10), inflammatory infiltration of eosinophils, and excess mucus secretion. Treatment with anti-Fc ϵ RI α Fab-NMs-celastrol efficiently alleviated

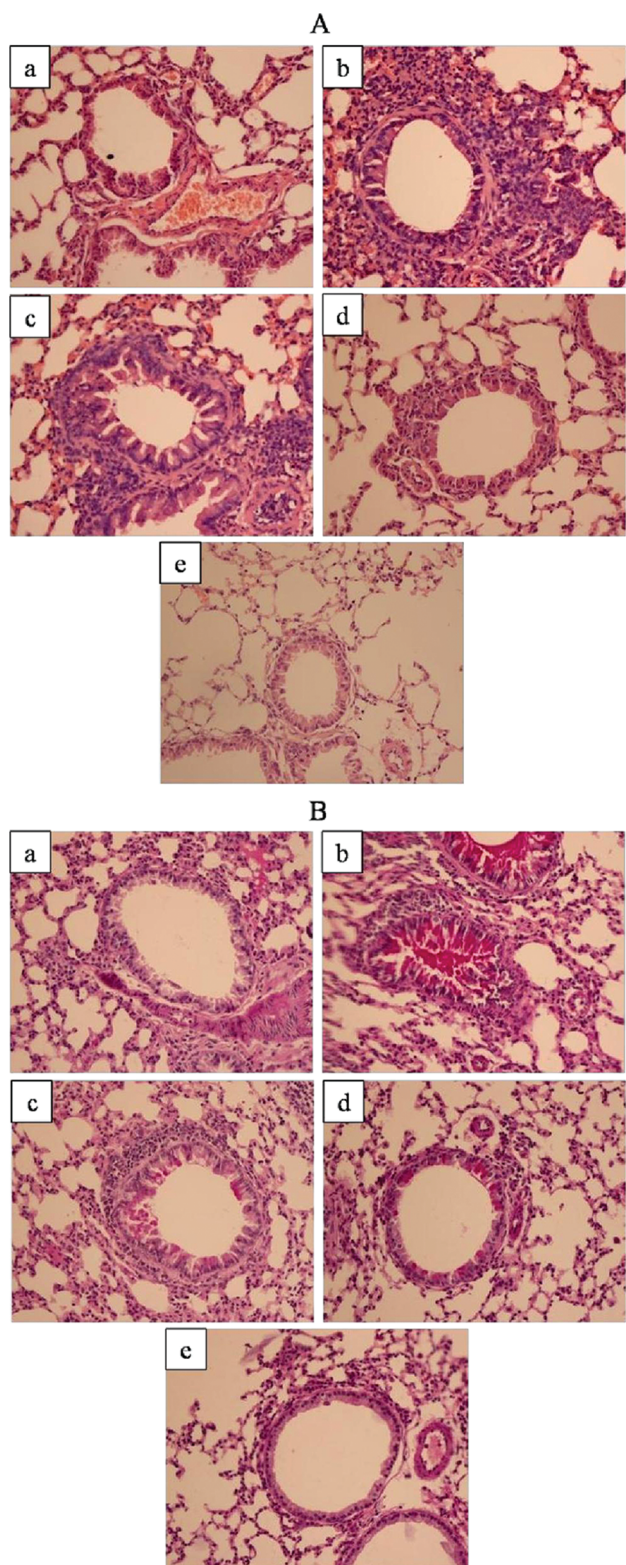


Figure 9. Histopathologic changes in the lung tissues. H and E (A) and PAS (B) staining of the lung tissues derived from non-sensitized mice treated with PBS (a), sensitized mice treated with PBS (b), sensitized mice treated with celastrol (c), sensitized mice treated with celastrol-NMs (d), sensitized mice treated with anti-Fc ϵ RI α Fab-NMs-celastrol (e). All images were captured at 20 \times magnification.

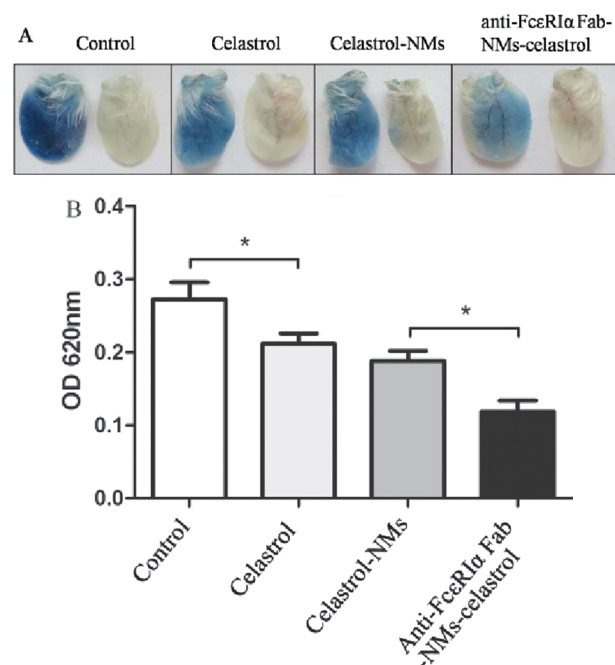


Figure 10. Effect of different celastrol formulations on IgE-mediated mast cell-dependent passive cutaneous anaphylaxis (PCA). Mice were treated with PBS, celastrol, celastrol-NMs, and anti-Fc ϵ RI Fab-NMs-celastrol intravenously at the celastrol concentration of 1.5 mg/kg, and then PCA model was performed. The dye extravasated was extracted from the ear and the amount was measured by absorbance at 620 nm. The representative photograph of ears (A) and the OD values (B) are shown (* p < 0.05, mean \pm SD, n = 5).

the pulmonary allergic inflammation in mouse model of allergic asthma.

To further confirm the anti-allergic effect of micelles, we investigated the inhibition of micelles on passive cutaneous anaphylaxis. Acute passive cutaneous anaphylaxis reaction induced by antigen in IgE-sensitized mice is mediated mainly by histamine released from activated mast cells.^{40,41} In PCA, allergic reaction occurs locally at the site of IgE injection in the skin and will lead to measurable extravasation. Our results demonstrated that treatment with anti-Fc ϵ RI α Fab-NMs-celastrol was effective in decreasing extravasation of Evans' blue, which indicated that anti-Fc ϵ RI α Fab-NMs-celastrol could relieve PCA reactions.

Consistent with *in vitro* apoptotic and *in vivo* biodistribution, the anti-Fc ϵ RI α Fab-conjugated micelles exhibited a higher anti-allergic effect than both non-conjugated micelles and native celastrol. Such increased efficacy of micelles could be explained by several factors. Indeed, anti-Fc ϵ RI α Fab-conjugated micelles

- (1) induced blood longevity of the drug,
- (2) decreased the urinary excretion of the drug,
- (3) increased accumulation of the drug within the target tissues and cells, and

(4) inhibited cell degranulation by competing with serum IgE for IgE high affinity receptor (FcεRIα) on mast cells and basophils.

At present, the major groups of drugs used in the treatment of allergic disorders are β -agonists, glucocorticoids, antihistamines and chromolyn sodium. Yet these drugs are not mast cell-specific, they do not prevent the allergic reaction, but only reverse or block its effects. Moreover, they cause serious side-effects to normal organs. The omalizumab, a humanized monoclonal anti-IgE antibody, also did not exhibit the desired effect for the large dosage and long therapy course.⁴² The anti-FcεRIα Fab-conjugated celastrol-loaded micelles may have a number of advantages over the existing drugs. As it affects mast cells and basophils, it could inhibit allergic inflammation fundamentally by eliminating the source of allergic mediators. Moreover, the micelles are expected to have few side-effects, as the FcεRI receptor is of restricted distribution.

In conclusions, the data shown in this article suggest that anti-FcεRIα Fab-conjugated celastrol-loaded nanomicelles exhibit the potential to specially induce mast cells and basophils apoptosis *in vitro* and to inhibit allergic inflammation *in vivo*. Thus, it may be a promising nano-drug for effective therapy of allergic diseases. Moreover, mast cells have been demonstrated to be implicated in various pathologic conditions such as systemic mastocytosis, solid tumor and chronic inflammatory diseases, including scleroderma and rheumatoid arthritis.^{43–46} Thus, targeted elimination of mast cells by the anti-FcεRIα Fab-conjugated celastrol-loaded micelles should have broad clinical applications.

Acknowledgments: This work was supported by the National Natural Science Foundation (No. 81471593, 81273276, 81072448, and 31100717), Science and Technology Commission of Shanghai Yangtze River Delta Technology joint research project (10495810200), Clinical Auxiliary Departments Construction Project of Shanghai Shen-Kang Hospital Development Center (SHDC22014005), Shanghai Natural Science fund (14411963200), the Innovation Plan of Shanghai Science and Technology (11JC1410300), and Specialized Research Fund for the Doctoral Program of Higher Education (No. 20110073120072). The authors appreciate the support by the Professor Daxiang Cui from Institute of Micro-Nano Science and Technology of Shanghai Jiao Tong University in the part for the samples preparation.

REFERENCES

1. R. Pawankar, G. W. Canonica, C. Stephen, and R. F. Lockey, White Book on Allergy 2011–2012: Executive Summary, World Allergy Organization, Milwaukee, Wisconsin, USA (2011), p. 1.
2. S. Kraft and J. P. Kinet, New developments in FcεRI RI regulation, function and inhibition. *Nat. Rev. Immunol.* 7, 365 (2007).
3. R. Belostotsky and H. Lorberbaum-Galski, Apoptosis-inducing human-origin Fc-Bak chimeric proteins for targeted elimination of mast cells and basophils: A new approach for allergy treatment. *J. Immunol.* 167, 4719 (2001).
4. A. Fishman and H. Lorberbaum-Galski, Targeted elimination of cells expressing the high-affinity receptor for IgE (Fc epsilon RI) by a *Pseudomonas* exotoxin-based chimeric protein. *Eur. J. Immunol.* 27, 486 (1997).
5. M. Li-Weber, Targeting apoptosis pathways in cancer by Chinese medicine. *Cancer Lett.* 332, 304 (2013).
6. T. W. Corson and C. M. Crews, Molecular understanding and modern application of traditional medicines: Triumphs and trials. *Cell* 130, 769 (2007).
7. D. Y. Kim, J. W. Park, D. Jeoung, and J. Y. Ro, Celastrol suppresses allergen-induced airway inflammation in a mouse allergic asthma model. *Eur. J. Pharmacol.* 612, 98 (2009).
8. Y. Bao, R. Yu, and D. Zhang, *In vitro* study on cellular and molecular mechanism of tripteryne treating leukemic mast cells. *Zhonghua Xue Ye Xue Za Zhi* 20, 146 (1999).
9. R. L. Liu, Z. L. Liu, Q. Li, Z. M. Qiu, H. J. Lu, Z. M. Yang, and G. C. Hong, The experimental study on the inhibitory effect of tripteryne on airway inflammation in asthmatic mice. *Zhonghua Jie He He Hu Xi Za Zhi* 27, 165 (2004).
10. A. Fishman, D. Prus, R. Belostotsky, and H. Lorberbaum-Galski, Targeted Fc2'-3-PE40 chimeric protein abolishes passive cutaneous anaphylaxis in mice. *Clin. Exp. Immunol.* 119, 398 (2000).
11. G. Gaucher, M. H. Dufresne, V. P. Sant, N. Kang, D. Maysinger, and J. C. Leroux, Block copolymer micelles: Preparation, characterization and application in drug delivery. *J. Control Release* 109, 169 (2005).
12. W. Xu, I. A. Siddiqui, M. Nihal, S. Pilla, K. Rosenthal, H. Mukhtar, and S. Gong, Aptamer-conjugated and doxorubicin-loaded unimolecular micelles for targeted therapy of prostate cancer. *Biomaterials* 34, 5244 (2013).
13. X. Peng, J. Wang, H. Song, D. Cui, L. Li, J. Li, L. Lin, J. Zhou, and Y. Liu, Optimized preparation of celastrol-loaded polymeric nanomicelles using rotatable central composite design and response surface methodology. *J. Biomed. Nanotechnol.* 8, 491 (2012).
14. R. Singh and J. W. Lillard, Nanoparticle-based targeted drug delivery. *Exp. Mol. Pathol.* 86, 215 (2009).
15. V. P. Torchilin, A. N. Lukyanov, Z. Gao, and B. Papahadjopoulos-Sternberg, Immunomicelles: Targeted pharmaceutical carriers for poorly soluble drugs. *Proc. Natl. Acad. Sci. U. S. A.* 100, 6039 (2003).
16. M. Yamaguchi, C. S. Lantz, H. C. Oettgen, I. M. Katona, T. Fleming, I. Miyajima, J. P. Kinet, and S. J. Galli, IgE enhances mouse mast cell Fc(epsilon)RI expression *in vitro* and *in vivo*: Evidence for a novel amplification mechanism in IgE-dependent reactions. *J. Exp. Med.* 185, 663 (1997).
17. A. Nechansky, M. W. Robertson, B. A. Albrecht, J. R. Apgar, and F. Kricek, Inhibition of antigen-induced mediator release from IgE-sensitized cells by a monoclonal anti-FcεRI α -chain receptor antibody: Implications for the involvement of the membrane-proximal α -chain region in FcεRI-mediated cell activation. *J. Immunol.* 166, 5979 (2001).
18. G. Kohler and C. Milstein, Continuous cultures of fused cells secreting antibody of predefined specificity. 1975. *J. Immunol.* 174, 2453 (2005).
19. H. Song, R. He, K. Wang, J. Ruan, C. Bao, N. Li, J. Ji, and D. Cui, Anti-H IF-1 alpha antibody-conjugated pluronic triblock copolymer encapsulated with paclitaxel for tumor targeting therapy. *Biomaterials* 31, 2302 (2010).
20. M. Shahin, S. Ahmed, K. Kaur, and A. Lavasanifar, Decoration of polymeric micelles with cancer-specific peptide ligands for active targeting of paclitaxel. *Biomaterials* 32, 5123 (2011).
21. X. Y. Li, L. J. Jiang, L. Chen, M. L. Ding, H. Z. Guo, W. Zhang, H. X. Zhang, X. D. Ma, X. Z. Liu, X. D. Xi, S. J. Chen, Z. Chen, and J. Zhu, RIG-I modulates Src-mediated AKT activation to restrain leukemic stemness. *Mol. Cell.* 53, 407 (2014).

22. L. H. Lin, P. Zheng, J. W. Yuen, J. Wang, J. Zhou, C. Q. Kong, X. Peng, J. Li, and L. Li, Prevention and treatment of allergic inflammation by an Fc γ -der f2 fusion protein in a murine model of dust mite-induced asthma. *Immunol. Res.* 52, 276 (2012).
23. K. D. Stone, C. Prussin, and D. D. Metcalfe, IgE, mast cells, basophils, and eosinophils. *J. Allergy Clin. Immunol.* 125, S73 (2010).
24. G. Marone, F. Granata, G. Spadaro, A. Genovese, and M. Triggiani, The histamine-cytokine network in allergic inflammation. *J. Allergy Clin. Immunol.* 112, S83 (2003).
25. M. Wills-Karp and C. L. Karp, Biomedicine. Eosinophils in asthma: Remodeling a tangled tale. *Science* 305, 1726 (2004).
26. T. C. Prathna, N. Chandrasekaran, A. M. Raichur, and A. Mukherjee, Biomimetic synthesis of silver nanoparticles by Citrus limon (lemon) aqueous extract and theoretical prediction of particle size. *Colloids Surf. B. Biointerfaces* 82, 152 (2011).
27. A. V. Kabanov, E. V. Batrakova, and V. Y. Alakhov, Pluronic block copolymers as novel polymer therapeutics for drug and gene delivery. *J. Control Release* 82, 189 (2002).
28. B. M. Jensen, J. B. Hansen, S. Dissing, J. Gerwien, P. S. Skov, and L. K. Poulsen, Monomeric immunoglobulin E stabilizes Fc epsilon RI alpha from the human basophil cell line KU812 by protecting it from natural turnover. *Clin. Exp. Immunol.* 33, 655 (2003).
29. S. Guhl, M. Babina, A. Neou, T. Zuberbier, and M. Artuc, Mast cell lines HMC-1 and LAD2 in comparison with mature human skin mast cells—drastically reduced levels of tryptase and chymase in mast cell lines. *Exp. Dermatol.* 19, 845 (2010).
30. Y. Wang, X. Wang, Y. Zhang, S. Yang, J. Wang, X. Zhang, and Q. Zhang, RGD-modified polymeric micelles as potential carriers for targeted delivery to integrin-overexpressing tumor vasculature and tumor cells. *J. Drug Target.* 17, 459 (2009).
31. S. K. Sahoo and V. Labhsetwar, Enhanced antiproliferative activity of transferrin-conjugated paclitaxel-loaded nanoparticles is mediated via sustained intracellular drug retention. *Mol. Pharm.* 2, 373 (2005).
32. A. S. Mikhail and C. Allen, Block copolymer micelles for delivery of cancer therapy: Transport at the whole body, tissue and cellular levels. *J. Control Release* 138, 214 (2009).
33. H. Jiang, P. Hener, J. Li, and M. Li, Skin thymic stromal lymphopoietin promotes airway sensitization to inhalant house dust mites leading to allergic asthma in mice. *Allergy* 67, 1078 (2012).
34. K. Nemeth, A. Keane-Myers, J. M. Brown, D. D. Metcalfe, J. D. Gorham, V. G. Bundoc, M. G. Hodges, I. Jelinek, S. Madala, S. Karpati, and E. Mezey, Bone marrow stromal cells use TGF-beta to suppress allergic responses in a mouse model of ragweed-induced asthma. *Proc. Natl. Acad. Sci. U. S. A.* 107, 5652 (2010).
35. J. M. Brown, T. M. Wilson, and D. D. Metcalfe, The mast cell and allergic diseases: Role in pathogenesis and implications for therapy. *Clin. Exp. Allergy* 38, 4 (2008).
36. S. Li, M. Aliyeva, N. Daphtary, R. A. Martin, M. E. Poynter, S. F. Kostin, J. L. van der Velden, A. M. Hyman, C. S. Stevenson, J. E. Phillips, and L. K. Lundblad, Antigen-induced mast cell expansion and bronchoconstriction in a mouse model of asthma. *Am. J. Physiol. Lung Cell Mol. Physiol.* 306, L196 (2014).
37. Y. Wang, Y. Li, L. Zhang, and X. Fang, Pharmacokinetics and biodistribution of paclitaxel-loaded pluronic P105 polymeric micelles. *Arch. Pharm. Res.* 31, 530 (2008).
38. P. Bradding, A. F. Walls, and S. T. Holgate, The role of the mast cell in the pathophysiology of asthma. *J. Allergy Clin. Immunol.* 117, 1277 (2006).
39. E. C. Cates, R. Fattouh, J. Wattie, M. D. Inman, S. Goncharova, A. J. Coyle, J. C. Gutierrez-Ramos, and M. Jordana, Intranasal exposure of mice to house dust mite elicits allergic airway inflammation via a GM-CSF-mediated mechanism. *J. Immunol.* 173, 6384 (2004).
40. E. Mertsching, L. Bafetti, H. Hess, S. Perper, K. Giza, L. C. Allen, E. Negrou, K. Hathaway, B. Hopp, J. Chung, D. Perret, M. Shields, A. Saxon, and M. R. Kehry, A mouse Fc gamma-Fc epsilon protein that inhibits mast cells through activation of Fc gamma RIIB, SH2 domain-containing inositol phosphatase 1, and SH2 domain-containing protein tyrosine phosphatases. *J. Allergy Clin. Immunol.* 121, 441 (2008).
41. J. I. Kashiwakura, T. Ando, K. Matsumoto, M. Kimura, J. Kitaura, M. H. Matho, D. M. Zajone, T. Ozeki, C. Ra, S. M. MacDonald, R. P. Siraganian, D. H. Broide, Y. Kawakami, and T. Kawakami, Histamine-releasing factor has a proinflammatory role in mouse models of asthma and allergy. *J. Clin. Invest.* 122, 218 (2012).
42. C. BuBmann, T. Bieber, and N. Novak, Systemic therapeutic options for severe atopic dermatitis. *J. Dtsch. Dermatol. Ges.* 7, 205 (2009).
43. E. C. Chan, Y. Bai, A. S. Kirshenbaum, E. R. Fischer, O. Simakova, G. Bandara, L. M. Scott, L. B. Wisch, D. Cantave, M. C. Carter, J. C. Lewis, P. Noel, I. Maric, A. M. Gilfillan, D. D. Metcalfe, and T. M. Wilson, Mastocytosis associated with a rare germline KIT K509I mutation displays a well-differentiated mast cell phenotype. *J. Allergy Clin. Immunol.* 134, 178 (2014).
44. J. Kalesnikoff and S. J. Galli, New developments in mast cell biology. *Nat. Immunol.* 9, 1215 (2008).
45. C. Louvet, G. L. Szot, J. Lang, M. R. Lee, N. Martinier, G. Bollag, S. Zhu, A. Weiss, and J. A. Bluestone, Tyrosine kinase inhibitors reverse type 1 diabetes in nonobese diabetic mice. *Proc. Natl. Acad. Sci. U.S.A.* 105, 18895 (2008).
46. Y. Ma, R. F. Hwang, C. D. Logsdon, and S. E. Ullrich, Dynamic mast cell-stromal cell interactions promote growth of pancreatic cancer. *Cancer Res.* 73, 3927 (2013).